Toxicology Reports 3 (2016) 747–755

Contents lists available at ScienceDirect

Toxicology Reports

journal homepage: www.elsevier.com/locate/toxrep

Targeted metabolomic profiling indicates structure-based perturbations in serum phospholipids in children with acetaminophen overdose

Sudeepa Bhattacharyya[a,b,*], Lisa Pence[c], Ke Yan[d], Pritmohinder Gill[a], Chunqiao Luo[a], Lynda G. Letzig[a], Pippa M. Simpson[d], Gregory L. Kearns[a], Richard D. Beger[c], Laura P. James[a]

[a] Department of Pediatrics, University of Arkansas for Medical Sciences, Little Rock, AR 72202, USA
[b] Arkansas Children's Research Institute, Little Rock, AR 72202, USA
[c] Division of Systems Biology, National Center for Toxicological Research, Jefferson, AR 72079, USA
[d] Medical College of Wisconsin, Milwaukee, WI 53226, USA

ARTICLE INFO

Article history:
Received 13 March 2016
Received in revised form 17 August 2016
Accepted 18 August 2016
Available online 23 August 2016

Keywords:
Metabolomics
Phospholipids
Acetaminophen
Hepatotoxicity
Drug

ABSTRACT

Phospholipids are an important class of lipids that act as building blocks of biological cell membranes and participate in a variety of vital cellular functions including cell signaling. Previous studies have reported alterations in phosphatidylcholine (PC) and lysophosphatidylcholine (lysoPC) metabolism in acetaminophen (APAP)-treated animals or cell cultures. However, little is known about phospholipid perturbations in humans with APAP toxicity. In the current study, targeted metabolomic analysis of 180 different metabolites including 14 lysoPCs and 73 PCs was performed in serum samples from children and adolescents hospitalized for APAP overdose. Metabolite profiles in the overdose group were compared to those of healthy controls and hospitalized children receiving low dose APAP for treatment of pain or fever (therapeutic group). PCs and lysoPCs with very long chain fatty acids (VLCFAs) were significantly decreased in the overdose group, while those with comparatively shorter chain lengths were increased in the overdose group compared to the therapeutic and control groups. All ether linked PCs were decreased in the overdose group compared to the controls. LysoPC-C26:1 was highly reduced in the overdose group and could discriminate between the overdose and control groups with 100% sensitivity and specificity. The PCs and lysoPCs with VLCFAs showed significant associations with changes in clinical indicators of drug metabolism (APAP protein adducts) and liver injury (alanine aminotransferase, or ALT). Thus, a structure-dependent reduction in PCs and lysoPCs was observed in the APAP-overdose group, which may suggest a structure-activity relationship in inhibition of enzymes involved in phospholipid metabolism in APAP toxicity.

1. Introduction

Acetaminophen (APAP, Tylenol®) is a widely used analgesic and antipyretic drug. Although generally considered safe when used at doses recommended by the manufacturer, APAP overdose is one of the most common causes of poison-related hospitalizations and acute hepatic failure in the western world [9,29]. Many reviews have summarized the current knowledge about the contribution of APAP metabolism to the generation of hepatotoxicity [18,48,22,33]. Briefly, hepatic metabolism of APAP by phase II conjugation produces nontoxic glucuronide and sulphate metabolites. A small amount of APAP undergoes CYP P450 oxidation [6,16,12] to form the highly reactive metabolite *N*-acetyl-*p*-benzoquinone imine (NAPQI), which is detoxified by hepatic glutathione (GSH). However, with APAP overdose and saturation of conjugation, high levels of NAPQI result in depletion of hepatocellular GSH and covalent binding of NAPQI to macromolecules, including cytosolic and mitochondrial proteins [34,36] giving rise to APAP protein adducts.

* Corresponding author at: Department of Pediatrics, University of Arkansas for Medical Sciences, Little Rock, AR 72202, USA.
E-mail addresses: SBhattacharyya2@uams.edu (S. Bhattacharyya), Lisa.Pence@fda.hhs.gov (L. Pence), kyan@mcw.edu (K. Yan), PSGill@uams.edu (P. Gill), CLuo@uams.edu (C. Luo), LetzigLyndaG@uams.edu (L.G. Letzig), psimpson@mcw.edu (P.M. Simpson), KearnsGL@archildrens.org (G.L. Kearns), Richard.beger@fda.hhs.gov (R.D. Beger), JamesLauraP@uams.edu (L.P. James).

http://dx.doi.org/10.1016/j.toxrep.2016.08.004

Other contributory events include mitochondrial dysfunction, ATP depletion, generation of reactive oxygen and nitrogen species, and apoptotic signaling [15,17,18,22]. Finally, other key events follow the initial insult such as inflammation, repair and hepatic regeneration, all of which play a major role in the outcome of APAP-induced hepatotoxicity [33]

Even though mechanisms of APAP toxicity have been widely studied, few investigations have examined the role of phospholipid homeostasis and disruption in APAP liver injury. Several experimental studies in animals and cell cultures have reported a depletion of phospholipids, suggesting either the inhibition of enzymes involved in phospholipid synthesis and/or an increase in activity of hepatic phospholipases in APAP toxicity. In 2003, Coen et al. [4] reported the depletion of phospholipid species in the livers of mice treated with toxic doses of APAP, suggesting the involvement of free radical damage or lipid peroxidation. Cheng et al. [3] reported lower levels of several lysophosphatidylcholine (lysoPC) species, lysoPC-C20:4, -C18:0, -C20:3, -C22:6 and -C18:3, in the serum of mice treated with toxic doses of APAP. Of the observed perturbations, LysoPC-C20:4 arachidonic acid (AA) was identified as the major metabolite that decreased in association with increasing hepatotoxicity. Two studies [10,43] used a rat model of APAP toxicity and reported lower levels of serum and hepatic phospholipids with concurrent increases in free fatty acids. Baseline levels of the metabolites were restored upon pre-treatment of the animals with hepato-protective compounds like methanolic extract of *Asteracantha longifolia* seeds and extract of *Premna tomentosa* [10,43]. Despite these findings, little is known about the underlying molecular mechanisms that drive phospholipid perturbations in APAP toxicity.

To describe and further elucidate the role of phospholipids in APAP toxicity in humans, we examined changes in serum phospholipids in response to APAP exposure and the relationship of these changes with clinical indicators of hepatotoxicity in children with APAP overdose. Targeted metabolomic analyses of 180 metabolites, including 87 different phospholipid species,14 lysoPCs and 73 PCs, was performed using serum samples in three groups: (a) hospitalized children receiving low dose acetaminophen for treatment of pain or fever, (b) healthy controls and (c) children and adolescents hospitalized for APAP overdose. Phospholipid profiles were compared to ALT (alanine aminotransferase), the clinical indicator of liver injury, and to APAP protein adducts [34], an indicator of oxidative metabolism.

2. Materials and methods

2.1. Study population

This was a multicenter study of APAP toxicity in children aged 2–18 years that was approved by the institutional review boards of all participating institutions. Following informed consent and assent when age appropriate, blood samples were collected from study subjects. As noted in two previous publications from this study cohort [1,23], the study included three subject subgroups as follows: group A (therapeutic dose group), defined as hospitalized children receiving APAP per standard of care; group B (control group), defined as healthy children with no use of APAP in the preceding 14 days; and group C (overdose group), defined as children requiring hospitalization for treatment of APAP overdose. Hospitalization of children with APAP overdose was determined according to published guidelines and included history of excessive dosing of APAP of >150 mg/kg and elevation of APAP concentrations in peripheral blood, plotted as a function of the time elapsed from the time of the overdose [24].

2.2. Sample collection

For subjects in group A, blood samples were collected prior to receipt of the first APAP dose 'on study' and thereafter at 8 and 24 h after the first dose of APAP, followed by convenience sampling throughout the period of hospitalization. APAP dosing, route and frequency were at the discretion of the treating physician for subjects in group A. A single blood sample was collected in group B subjects and admission and daily morning blood samples were collected in subjects in group C. All samples were collected in accordance with a Manual of Operations and Procedures developed for the study. For each sample collection, 1.5 ml of whole blood was obtained in a 5 ml red-top tube. The tube was inverted 8–10 times; and the sample was allowed to clot at room temperature for 30 min and centrifuged at <1300 RCF for 10 min at 4 °C. The resulting serum was aliquoted into cryovials and frozen at −70 ° within one hour for future batch analysis.

For all subjects that had sera collected at multiple time points per group, APAP adducts, ALT and metabolite levels were assayed at each time point and the peak values for each of the parameters were considered for downstream statistical analysis.

2.3. Clinical data

Demographic (age, gender, race, weight and height), clinical (APAP dose, route, dose interval, *N*-acetylcysteine dose, route, cumulative dose and reason for hospitalization) and laboratory data (serum ALT and international normalized ratio [INR] for prothrombin time) were recorded in a specific database designed for the study [24].

2.4. Clinical chemistry

Circulating levels of APAP protein adducts have been established as a biomarker of APAP toxicity in experimental models and clinical samples [8,34]. Serum samples were analyzed for APAP protein adducts by high-performance liquid chromatography with electrochemical detection (HPLC-EC) as previously reported [8,34]. Measurement of serum ALT was performed in the clinical chemistry laboratories at the participating institutions using standardized methods.

2.5. Metabolomics analysis

The Absolute-IDQ® platform (p180 kit, Biocrates Life Sciences AG, Austria) was employed for targeted metabolite profiling as described by the manufacturer. This platform detects a total of 180endogenous metabolites, including 30 amino acids and biogenic amines, 40 acylcarnitines (Cx:y), hydroxylacylcarnitines (C (OH) x:y) and dicarboxylacylcarnitines (Cx:y-DC), the sum of hexoses, 14 sphingomyelins (SMx:y) and sphingomyelin derivatives (SM (OH) x:y), 9 bile acids as well as 14 lyso-phosphatidylcholines (lysoPC) and 73 phosphatidylcholines (PC). The phospholipids are further sub-categorized with respect to the presence of an ester ("a") or an ether ("e") linkage in the glycerol moiety. The two letters "aa" (=diacyl) and "ae" (=acyl-alkyl) indicate that two glycerol positions are bound to a fatty acid residue, while a single letter "a" (=acyl) indicates the presence of a single fatty acid residue. The lipid side chain composition is abbreviated with "Cx:y", where "x" denotes the number of carbons in the side chain and "y" the number of double bonds [21]. A detailed list of all analyzed metabolites has been published [20,46].

The identification of lipids in Biocrates technology is based on the specific fragmentation of lipids in the triple quadrupole mass spectrometer, i.e. multiple reaction monitoring (MRM) in the tandem MS–MS. The transitions, from parent ions (M+H) to daugh-

Table 1
Demographic and Clinical Data, presented as median (range).

	Group A (Therapeutic) N = 8	Group B (Control) N = 19	Group C (Overdose) N = 16
Age (years)*	13.83 (9.33, 17.75)	9.00 (2.67, 16.17)	15.75 (1.50, 18.25)
Weight (kg)*	60.90 (11.60, 98.70)	40.80 (11.40, 99.80)	63.55 (10.00, 117.20)
Sex (% Male)	73.3	31.6	21.9
Peak ALT (IU/L)*	33.5 (7.00, 55)	16.5 (10.00, 37.00)	1827 (21.00, 2396.31)
Peak Adduct* (nmol/mL)	0.23 (0.05, 2.11)	0.006 (0.00, 0.01)	1.13 (0.50, 7.92)

* Statistically significant (Kruskal-Wallis test p-value <0.05).

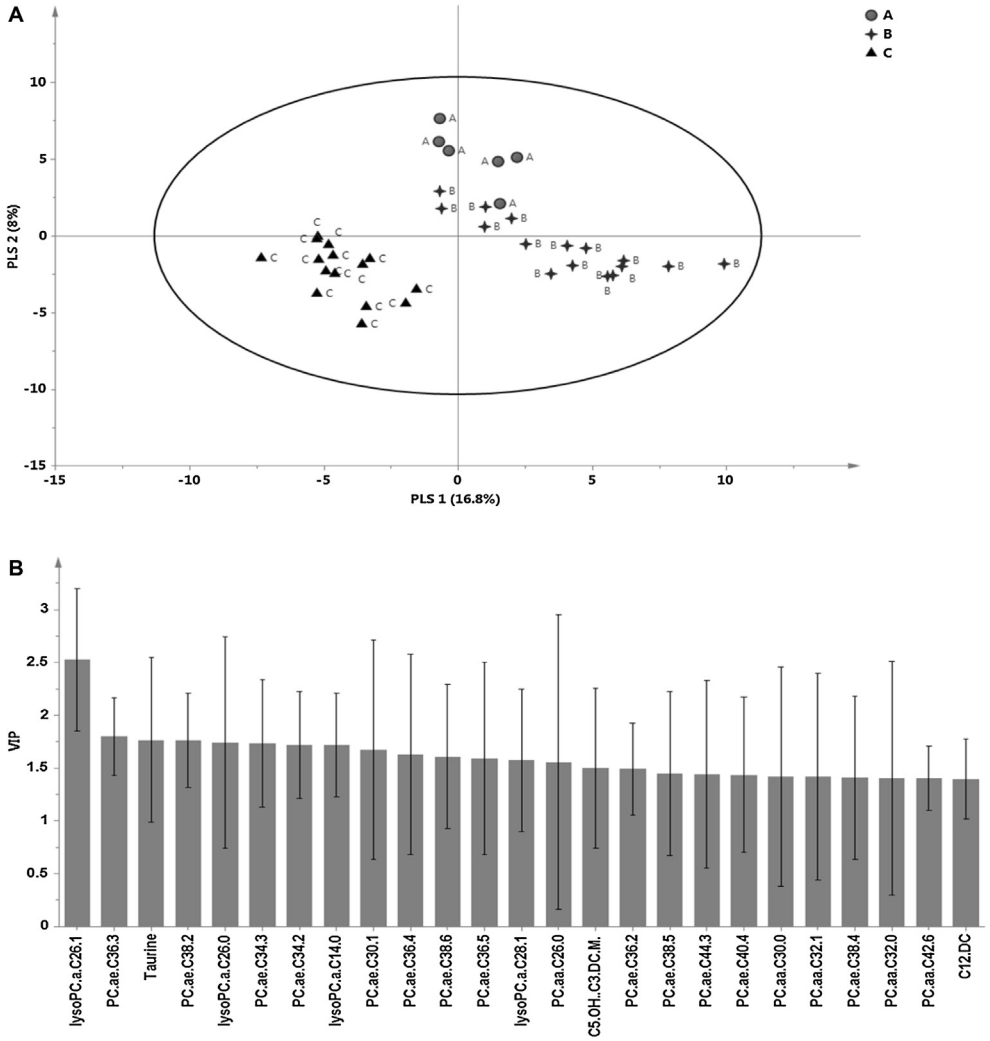

Fig. 1. Partial least squares discriminant analysis model. A) scores plot showing separation between the three subject groups, A (therapeutic), B (control) and C (overdose) along the first two PLS components. B) The top 25 metabolites based on the variable importance on the projection (VIP) values of the PLSDA model. The error bars around the VIP scores represent jack-knifing uncertainties.

ter ions, applied here are selective for the classes of compounds targeted in the Kit. Waters' ACQUITY UPLC® System with Xevo triple-quadrupole mass spectrometer (Waters, MA, USA) combined with the AbsoluteIDQ® p180 Kit was used for rapid and quantitative analyses by stable isotope dilution mass spectrometric analysis. The kit contains a 96-deep-well plate with filter plate attached and sealed, and includes isotope-labeled internal standards and seven calibrators sufficient for quantitation of metabolites and three levels of quality control samples (low, medium and high concentration spiked human plasma). The chromatographic separation was carried out using a Waters BEH C18 UPLC Column (2.1 × 50 mm, 1.7-μm particle size). Mobile phase A was 0.2% formic acid in water (Fisher Optima grade). Mobile phase B was 0.2% formic acid in acetonitrile (Fisher Optima grade). Analytes were detected on a Xevo triple quadrupole mass spectrometer operated in positive electrospray ionization mode with a capillary voltage of 3.3 kV. The source temperature was 150 °C, the desolvation temperature was 400 °C and the desolvation gas flow rate was 700L/h. Data was processed using Mass Lynx v. 4.1 (Waters) and imported into the MetIDQ software (Biocrates) for further analysis and validation. The limit of detection (LOD) was calculated from the average of zero samples (PBS, Sigma-Aldrich) run in triplicate with each individual 96 well plate. For statistical analyses, only metabolites were chosen for which metabolite concentrations exceeded the mass spectrometer detection limit. For the quantitative analytes (amino acids and biogenic amines), the concentrations were extrapolated from the calibration curve generated using the seven level calibrators provided in the AbsoluteIDQ® p180 Kit.

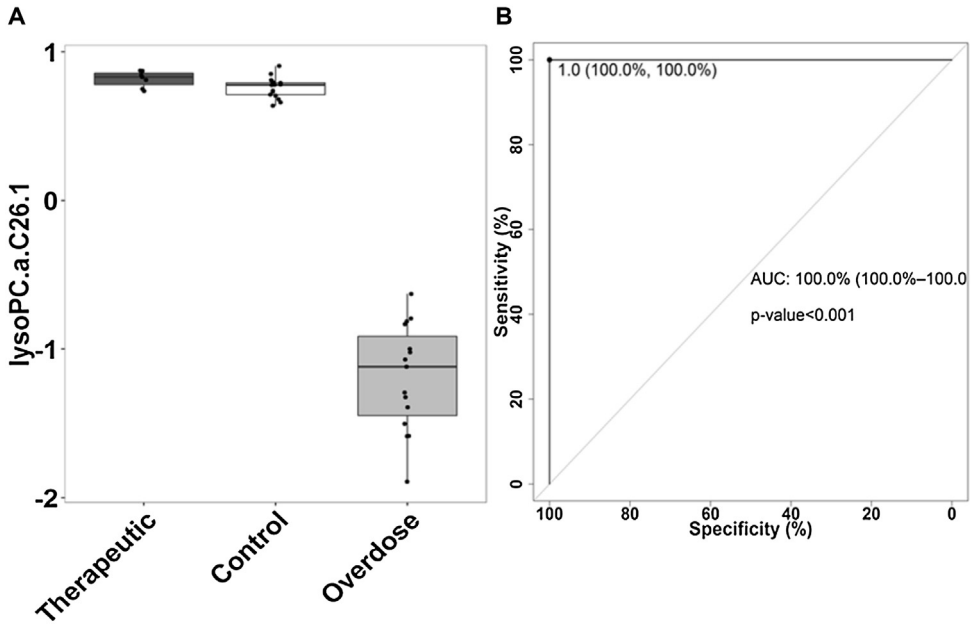

Fig. 2. (A) Boxplot showing changes in lysoPC-C26:1 in the APAP overdose and the therapeutic groups compared to controls. (B) ROC plot identified a cut-point of 0.9 UM (sensitivity 100%; specificity 100%) for lysoPC-C26:1, with an AUC of 1 (p-value <0.001) in discriminating the overdose from the control group.

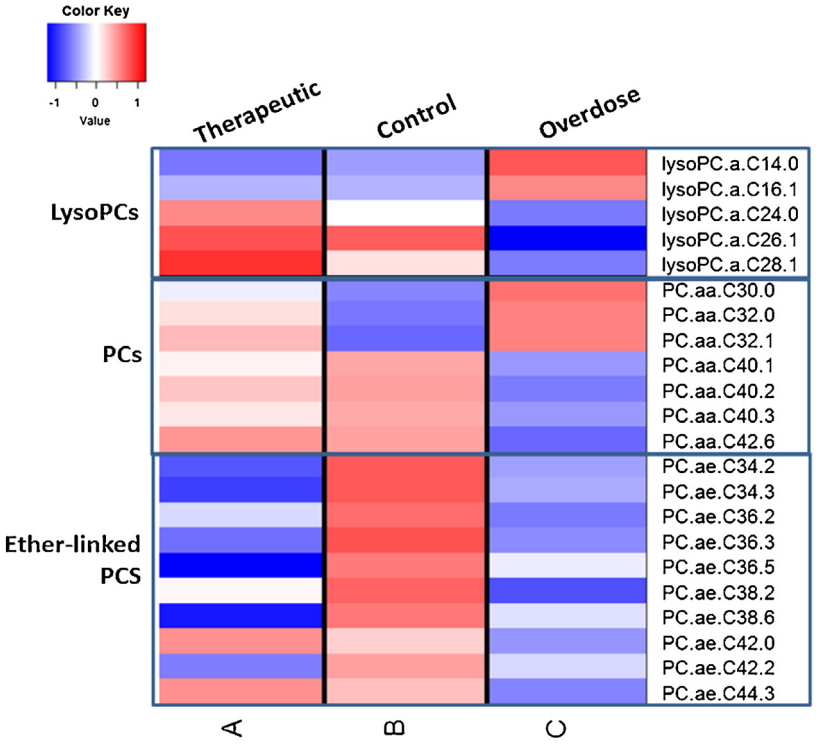

Fig. 3. A heatmap showing the changes in median concentrations (in log2 scale) in the three classes of phospholipids, lysoPCs, PCs and ether-linked PCs among the three subject groups.

2.6. Statistical analysis

Since samples over multiple time points were obtained for the study subjects in Groups A and C, the data were analyzed by peak measured value for ALT, APAP protein adducts, and metabolites [1,23–25]. The non-parametric Kruskal-Wallis test followed by post-hoc Dunn's test was used to compare analytes between the three subject groups. The Mann Whitney U Test was used for pairwise comparisons for ALT and APAP protein adducts. Spearman rank correlation coefficients were calculated to assess the relationship between ALT, APAP protein adducts and endogenous metabolites. A p value <0.05 was considered to be statistically 'significant' for all analyses. A receiver operating characteristic (ROC) analysis was performed on the most significantly changing metabolite to assess its performance as a binary classifier. All statistical analyses were performed by the open source statistical software package R. Multivariate data analysis was performed using the R package chemometrics [45] and SIMCA-P+ software (Umetrics,

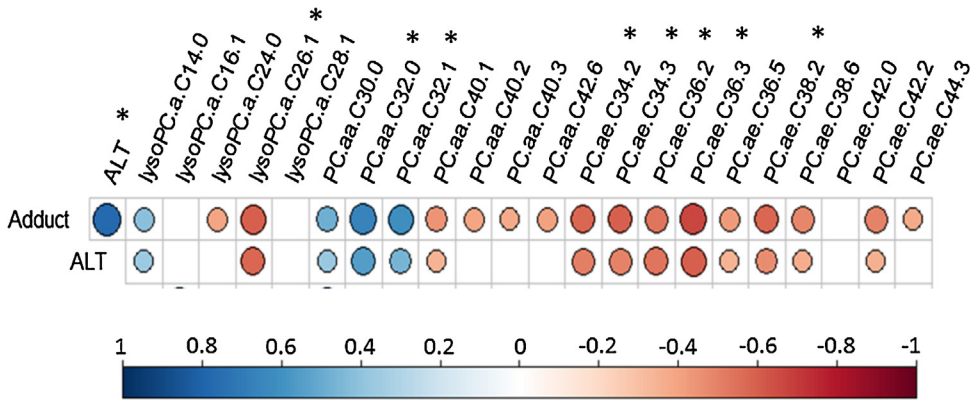

Fig. 4. Correlation plot showing Spearman Rank correlations between ALT, Adduct and the 22 significantly changing phospholipids. * represent phospholipids with moderate to high correlation coefficients ($R > 0.5$ or $R < -0.5$, $p < 0.05$). The larger the circle size the higher is the correlation coefficient. Cells with missing circles are statistically non-significant. n.

Kinnelon, NJ, USA). The data matrix was transformed by autoscaling and a final partial least squares discriminant analysis (PLS-DA) model was generated to identify metabolites that closely associated with the toxicity status. Major latent variables in the data were represented in a scores scatter-plot and the significant predictors were identified by their contribution to the PLS vectors in the loadings scatter plot as well as based on their variable importance on the projections (VIP) scores.

3. Results

3.1. Clinical and demographic data

Serum samples from a total of 43 children (Group A or therapeutic dose group, 8 subjects with multiple time points; Group B or healthy control group, 19 subjects with a single time point; Group C or APAP overdose group, 16 subjects with multiple time points post overdose exposure) were evaluated for metabolites using the Biocrates p180 kit. Table 1 summarizes the demographic and clinical parameters of the study subjects. Children in the three groups varied significantly with respect to age and sex. The children in group B were younger (median age: 9 years) than those of groups A and C (median ages, 13.83 years and 15.75 years respectively) and hence, had lower body weights. Groups B and C had more females (68.4% and 78.1% respectively) than group A. The subjects in the three groups did not differ significantly with respect to race and/or ethnicity (data not shown). All patients in Group C were judged to be "at risk" for APAP toxicity based on the Rumack nomogram [1,23], and/or elevations of ALT and other clinical factors, such as co-ingestion of drugs altering gastric motility at the time of presentation to the hospital. In group C, 9 out of 16 subjects (56.3%) had ALT values >1000 IU/L. All subjects in group C received treatment with the antidote, N-acetylcysteine (NAC). No deaths or liver transplants occurred in the study cohort.

3.2. Changes in ALT and APAP protein adducts by APAP exposure group

Summary data for ALT and APAP protein adducts are also provided in Table 1. No significant differences were detected by pairwise comparisons in median ALT values between group A and group B (Table 1). However, median levels of ALT and APAP protein adducts were significantly higher in group C than in groups A and B, and consistent with previous data, [1] significant correlations with ALT and APAP protein adducts were observed in group C ($R^2 = 0.78$, $p < 0.05$; Fig. 4).

3.3. Changes in serum phospholipids by group

A multivariate Partial Least Squares-Discriminant Analysis (PLS-DA) model revealed clear separation between the three groups of children. Group C clearly separated from the other groups (Fig. 1A), consistent with greater toxicity (elevated ALT and APAP protein adducts) in this group. The optimum six-component PLS-DA model captured approximately 56.4% of the variation in X variables (predictor variables: all metabolites) that correlated with approximately 97% of variation in the three groups. The goodness-of-predictability parameter (Q^2), calculated by a seven-round internal cross-validation of the data, was approximately 77%. The model was further validated by repeated permutations ($n = 1000$) of the sample identifiers and a reference distribution of all R^2 and Q^2 values from the permuted PLSDA models were vetted against the actual model. The final PLSDA model was only accepted if the estimated probability of the candidate model randomly occurring was significantly low ($p < 0.05$). The top 25 metabolites based on VIP values are shown in Fig. 1B.

Twenty two out of the top twenty five significant metabolites (or 88%) with VIP values >1 were the phospholipids, PCs and lysoPCs. All 22 PCs and lysoPCs showed significant changes in the overdose group compared to the control group, while 8 of 22 were also significantly different in the therapeutic dose group compared to control group. In addition, 7 of 22 metabolites showed significant differences between the therapeutic and overdose groups. Summary data of peak values of the 22 metabolites found to be statistically significant by both multivariate and univariate analyses are presented in Table 2. The metabolite that most clearly discriminated among the overdose and control groups was lysoPC-C26:1. A boxplot showing the median changes in lysoPC-C26:1 in the three groups is presented in Fig. 2A. ROC curve (Fig. 2B) analysis of lysoPC-C26:1 identified a cut-point of 0.9 UM (sensitivity 100%; specificity 100%) for this metabolite, with an AUC of 1 for discriminating the overdose group from the control group.

3.4. Structural differences in the phospholipids associated with toxicity

Interestingly, among the significantly perturbed phospholipids, the lysoPCs with very long chain fatty acids (VLCFAs, >C20), namely, lysoPCs -C24:0, -C26:1 and -C28:1- were decreased, while those with comparatively shorter chain lengths ($\leq$C20) were increased in the overdose group compared to the therapeutic and control groups. This general trend was noticed among the lysoPCs, irrespective of whether statistically significant or not at $p < 0.05$. Similarly, PCs with VLCFAs $\geq$ C38 were decreased while those with relatively

Table 2
Summary data of peak values of the 22 phospholipids by subgroup, presented as median and range.

Phospho-lipids	Therapeutic (Gr A) (μM)	Control (Gr B) (μM)	Overdose (Gr C) (μM)	PLS-DA VIP	Kruskal-Wallis p_value	Dunn's test for Multiple comparisons (Benjamini-Hochberg adjusted p_value)		
						B-A	C-A	C-B
lysoPC a C14:0	1.97 (1.54–3.82)	2.02 (0.99–2.63)	3.41 (2.50–4.75)	1.72	<0.0004	NS*	<0.002	<0.002
lysoPC a C16:1	3.13 (1.65–4.41)	2.86 (0.01–4.99)	4.16 (2.78–7.19)	1.34	<0.03	NS	NS	<0.03
lysoPC a C24:0	0.43 (0.29–1.02)	0.38 (0.11–2.54)	0.28 (0.16–0.47)	1.20	<0.009	NS	<0.02	<0.02
lysoPC a C26:1	2.99 (2.68–3.45)	2.80 (1.20–3.22)	0.36 (0.15–0.76)	2.53	<0.0000008	NS	<0.00002	<0.00004
lysoPC a C28:1	0.99 0.83–1.59)	0.70 (0.11–1.65)	0.57 (0.35–0.92)	1.57	<0.002	<0.047	<0.002	<0.047
PC aa C30.0	2.79 (1.9–6.47)	2.26 (0.33–4.11)	3.35 (2.43–10.45)	1.42	<0.003	NS	NS	<0.002
PC aa C32.0	17.85 (12.57–49.03)	13.87 (0.11–42.20)	20.56 (12.79–46.67)	1.40	<0.003	<0.048	NS	<0.002
PC aa C32.1	20.07 (9.47–29.52)	10.42 (0.14–25.10)	18.65 (11.54–57.89)	1.42	<0.0007	<0.011	NS	<0.002
PC aa C40.1	0.44 (0.26–0.84)	0.45 (0.30–1.42)	0.34 (0.28–0.94)	1.25	<0.03	NS	NS	<0.022
PC aa C40.2	0.30 (0.26–0.82)	0.36 (0.05–1.88)	0.26 (0.12–0.35)	1.24	<0.007	NS	NS	<0.007
PC aa C40.3	0.44 (0.36–1.25)	0.47 (0.01–1.41)	0.40 (0.28–0.58)	1.16	<0.043	NS	NS	<0.04
PC aa C42.6	0.76 (0.65–1.27)	0.78 (0.52–1.96)	0.56 (0.39–0.89)	1.40	<0.003	NS	<0.009	<0.007
PC ae C34.2	7.77 (5.94–16.11)	11.55 (0.03–16.47)	8.62 (6.47–11.49)	1.72	<0.0004	<0.002	NS	<0.003
PC ae C34.3	5.20 (3.27–18.52)	10.38 (0.07–15.46)	6.01 (3.43–11.60)	1.73	<0.0001	<0.0007	NS	<0.0008
PC ae C36.2	12.70 (10.94–27.60)	14.51 (0.04–23.20)	10.49 (8.87–16.24)	1.49	<0.002	NS	NS	<0.0009
PC ae C36.3	5.78 (4.37–11.70)	9.15 (5.81–13.62)	6.13 (4.64–8.32)	1.80	<0.0001	<0.001	NS	<0.0005
PC ae C36.5	6.47 (4.2–35.65)	13.36 (0.04–38.27)	10.38 (6.80–18.20)	1.59	<0.0009	<0.0007	NS	<0.045
PC ae C38.2	1.95 (1.09–5.48)	1.98 (0.05–3.60)	1.25 (0.80–4.20)	1.76	<0.0004	NS	NS	<0.0006
PC ae C38.6	4.34 (2.70–15.58)	7.54 (0.03–11.54)	5.51 (3.76–8.60)	1.61	<0.002	<0.002	NS	<0.019
PC ae C42.0	0.63 (0.46–1.11)	0.58 (0.45–1.61)	0.47 0.38–0.87)	0.95	<0.022	NS	<0.03	<0.03
PC ae C42.2	0.33 (0.11–0.95)	0.38 (0.20–0.76)	0.29 (0.13–0.54)	1.23	<0.036	NS	NS	<0.045
PC ae C44.3	0.16 (0.05–0.33)	0.12 (0.01–0.25)	0.09 (0.03–0.21)	1.44	<0.01	NS	<0.03	<0.03

* NS represents non-significant p values.

shorter chain lengths ≤C36 were increased in overdose group compared to controls. Similar to lysoPCs, this trend was observed in the non-significant PCs too. All ether linked PCs were decreased in the overdose group compared to the controls. A heat map showing the changes in the different phospholipid classes in the three groups are presented in Fig. 3.

3.5. Correlations of phospholipids to indicators of toxicity

Spearman Rank correlation analyses of ALT and APAP protein adducts with serum phospholipids was performed in the overdose group (Fig. 4). Inverse correlations were observed for lysoPC a C26:1 with adducts ($R = -0.598$, $p < 8e\text{-}05$) and with ALT ($R = -0.574$, $p < 0.0002$). PC aa C32:0, PC aa C32:1 and the ether-linked phospholipids, PC ae C34:2, PC ae C34.3, PC ae C36.2, PC ae C36.3 and PC ae C38.2 also showed significant ($R > 0.5$ or $R < -0.5$, $p < 0.05$) correlations to adducts and ALT (Fig. 4).

To further examine the relationship of the highest discriminatory lipid (between the control and overdose group) lysoPC-C26:1 to toxicity, subjects were re-classified by APAP protein adduct status, as <1.0 nmol/mL or ≥1.0 nmol/mL. This threshold was previously identified to have excellent sensitivity and specificity (97 and 95%, respectively) in patients with APAP liver injury with an ALT value of >1000 IU/L [25]. ROC analysis determined that lysoPC-C26:1 >1 uM was the optimum threshold to maximize sensitivity and specificity, 81.8% and 78.8%, respectively, in discriminating groups classified by adduct level (Fig. 5 in supplement). Additionally, when the subjects were stratified by lysoPC-C26:1 <1 μM or lysoPC-C26:1 >=1 μM, APAP protein adduct and ALT levels were significantly different between the two groups ($p < 0.05$).

Overall, our data demonstrate that perturbations in lysophosphatidylcholines and phosphatidylcholines occur in APAP toxicity in children and vary as a function of fatty acid chain lengths. LysoPCs and PCs with comparatively shorter chain lengths were elevated while those with very long chain fatty acids or VLCFAs were decreased in the APAP overdose group. All ether phosphatidylcholines were decreased in the overdose group compared to controls. The PCs and lysoPCs with VLCFAs hadsignificant correlations to the markers of APAP toxicity and metabolism, ALT and APAP-adducts, respectively. Furthermore, a lysophosphatidylcholine, lysoPC-C26:1 was identified as a strong candidate biomarker for APAP toxicity.

4. Discussion

Phospholipids are important components of the cell membranes in all living tissues including the liver [11,28,44]. They contribute to the physicochemical properties of the membrane influencing the conformation and function of membrane-bound proteins like receptors, ion channels, and transporters. As well, they regulate cell function by serving as precursors for prostaglandins and other signaling molecules [44]. One of the major classes of phospholipids in mammals is phosphatidylcholine (PC). In addition to being the major structural component of cellular membranes including mammalian liver, PC serves as a reservoir for several bioactive lipids including the most abundant lysophosphatidylcholine (lysoPC) which can function as small signaling molecules regulating diverse physiological and pathological processes through G protein-coupled receptors [11,28]. LysoPC is known to participate in the processes of internal and external wound healing and organ regeneration as well as in the therapy of autoimmune and neurodegenerative diseases [11].

The chemical structure of PC consists of a polar head group with a choline and a phosphate group attached to two fatty acid residues via a glycerol moiety. LysoPCs are derived from PCs through partial hydrolysis and removal of one of the fatty acid residues by the enzymatic action of phospholipase A2. The carbon chain lengths of fatty acid residues, as well as their structural modifications in PCs and lysoPCs, have recently emerged as an important correlate of their biological functions [13,14,27]. Very few studies have reported phospholipid perturbations in APAP hepatotoxicity and to our knowledge, perturbations in phospholipids in APAP toxicity in humans have not been examined. Previous animal and cell culture studies reported lower levels of either total phospholipids [10,43] or lysoPCs containing long chain fatty acids (between 14 and 20 carbons) [3,13,14]. A novel finding of the current study was the relationship between fatty acyl chain length of lysoPCs and PCs and their serum profiles in children with APAP overdose exposure. That is, lysoPCs and PCs with very long chain fatty acids (VLCFAs) were decreased, while those with comparatively shorter chain lengths were increased. Fatty acid chain length-dependent perturbations in lysoPCs and PCs have been reported in several models of cellular dysfunction but, to our knowledge, not in APAP hepatotoxicity [13,27]. Moreover, few publications have addressed changes in lysoPCs with VLCFAs (>22 carbons) in cellular toxicity. Interestingly, similar to our findings, Imhasly et al. [21] recently reported an increase in PCs with relatively short chain fatty acids, PC aa C30:2 and PC aa C32:2, and reduction in PCs with larger fatty acid components (≥34 carbons) in cows with hepatic lipidosis.

Even though numerous biological effects are exerted by lysoPCs depending on their specific structural properties, little research has investigated the underlying cellular and molecular mechanisms that drive structure-dependent changes in biologic function. Possible postulations include (1) decreased synthesis of PC's due to hypoxia or defects in oxidative phosphorylation [32] or (2) increased utilization of PCs to repair damaged cell membranes and to act as antioxidants [5]. It has also been suggested that depletions of lysoPCs could occur through reduced phospholipase A2 activity affecting hydrolysis of PCs to lysoPCs [2] or reduced activity of lecithin:cholesterol acyltransferase (LCAT) which affects lysoPC production by transacylation of the sn-2 fatty acid residue of lecithin to free cholesterol [11]. In a recent study [31] of D-galactosamine induced fulminant hepatic failure, long chain PCs and lysoPCs were depleted and then were restored through stem cell transplantation. Thus, collectively, the data suggest that both PCs and lysoPCs play a significant functional role in global liver injury and/or the recovery process.

In the present study we observed significant changes in PCs and lysoPCs with VLCFAs. Indeed, VLCFAs, carried by the phospholipids, have been implicated in many functions not substituted by other long chain fatty acids, including regulating cellular functions by affecting structural properties of the membrane like membrane fluidity, permeability, curvature, and lipid microdomain formation [26,39]. It is possible that the dependency on the acyl chain length of the phospholipids may be related to the access or insertion process of the phospholipids to the membrane bilayers during hepatic regeneration [14].

One interesting finding of our study was the discriminatory effect of lysoPC-C26:1, a lysoPC with a VLCFA, among the control and overdose groups. This lysoPC was highly decreased in the overdose group (compared to the control or the therapeutic dose groups) and was statistically significant before and after adjusting for age and sex in logistic regression models. Interestingly, lysoPC-C26:0, the unsaturated native of lysoPC-C26:1, was recently reported as a candidate biomarker for X-linked adrenoleukodystrophy (X-ALD) [19] and other peroxisomal disorders of peroxisomal β-oxidation like Zellweger syndrome [41]. Indeed, APAP has been reported to directly or indirectly perturb peroxisomal activity and activation of PPAR-alpha, a major regulator of mitochondrial and peroxisomal β-oxidation is known to protect against APAP hepatotoxicity in the mouse model [35].

Both PCs and lysoPCs have been implicated in metabolic and inflammatory diseases such as diabetes, Alzheimer's disease, and pre-hypertension [11,27,42,47]. However little is known about the underlying mechanisms leading to changes in phospholipids in drug induced hepatotoxicity. Given the fact that APAP-induced toxicity has been mechanistically linked to mitochondrial dysfunction, oxidative stress, nitrogen stress, lipid peroxidation, increased inflammation and eicosanoid generation, it is possible that perturbations in PCs and lysoPCs are directly or indirectly linked to some or all of the above events. The perturbations may also be associated with the liver regeneration process through structure-based selective insertions in membrane bilayers. Nonetheless, further investigation of the role of perturbations in PCs and lysoPCs in APAP toxicity is warranted as the collective data, based on animal studies and our current study, suggest that these metabolites may be linked to mechanisms that regulate hepatocellular homeostasis.

Our results from this exploratory study have limitations common to small-scale cross-sectional and observational studies. We were able to evaluate associations of the metabolites to toxicity outcomes, rather than assessing prospective predictions. Group A subjects were heterogeneous both in APAP dosing (administered on an as needed basis) and medical conditions requiring hospitalization which may have contributed to the variability of observed phospholipids in this group. Another limitation of the study was that the sample collection schedules were aligned with clinically-indicated monitoring of APAP overdose. Due to the convenience sampling design of the study, the data points were analyzed relative to peak measurements of all analytes and biomarkers as has been reported previously [1,23–25]. The three subject groups differed somewhat by age and gender due to the nature of the study design and convenience sampling. In general, there is evidence in published literature that age and sex variation contributes to drug toxicity profiles. However, despite a massive experimental literature related to APAP, data on impact of age and gender on APAP-induced liver toxicity is pretty limited and drawn mostly from animal models or in vitro studies. There are few studies that have shown that older patients (>40 years of age) are at risk to develop APAP toxicity [40] while children less than five years old appear less susceptible to APAP toxicity due to increased rate of glutathione synthesis and greater activity of conjugation enzymes [30,37]. Adult patterns of APAP metabolism are reached between 10 and 12 years of age, in children [38]. In terms of sex differences in APAP-toxicity, female mice have been shown to be more resistant to APAP induced hepatotoxicity [7]. The sex-specific differences are poorly understood in molecular or cellular terms and are primarily thought to be due to fundamental physiological differences like pharmacokinetics/pharmacodynamics or hormones. Thus existing knowledge is sparse in terms of age or sex as confounders in APAP toxicity in humans, especially in the pediatric population and how it can impact phospholipid profiles. The differences in age and sex in our study population and its impact on the observed lipid differences need to be addressed in a future, larger study cohort. In addition, the observed changes in the phospholipids may have been influenced by nutritional status and other unknown environmental factors. In this study the nutritional status was not controlled for in any of the three groups due to the nature of the study design (i.e., a pediatric study involving hospitalized children in which control of diet would be difficult due to the variety of medical conditions of the children). Future studies in older populations using healthy subjects would allow for a more controlled evaluation of the relationship between nutritional status, APAP dose, and phospholipid perturbations. Despite these limitations, the findings of this study conducted in the "real world" setting of APAP toxicity and therapeutic exposure among ill children and adolescents does have similar findings to those observed in highly controlled experimental studies of APAP toxicity in rodents. One noted advantage of pediatric study populations is that they are in general devoid of long-term, chronic illnesses such as pre-existing liver disease (eg., non-alcoholic fatty liver disease) that would be a likely covariate of adult populations.

In conclusion, this study provides a proof-of-concept data to prompt further in-depth investigation of the role of phospholipids in drug-induced liver injury both from the perspective of dysfunction and evolving resolution of liver injury to normal homeostatic function. The structure based perturbations of the PCs and LPCs in APAP toxicity is a novel finding and needs to be further explored to better understand the functional and mechanistic implications of these endogenous metabolites in APAP hepatotoxicity.

Financial support and disclaimer

This work was funded in part by a grant (R01 DK75936 to LPJ) from the National Institutes of Diabetes, Digestive and Kidney Diseases and the Arkansas Biosciences Institute which is funded by Arkansas Tobacco Settlement Funds.

The views presented in this article are those of the authors and do not necessarily reflect those of the National Institutes of Health, the Arkansas Biosciences Institute or the United States Food and Drug Administration. No official endorsement is intended nor should be inferred.

Transparency document

The Transparency document associated with this article can be found in the online version.

Appendix A. Supplementary data

Supplementary data associated with this article can be found, in the online version, at http://dx.doi.org/10.1016/j.toxrep.2016.08.004.

References

[1] S. Bhattacharyya, K. Yan, L. Pence, P.M. Simpson, P. Gill, L.G. Letzig, R.D. Beger, J.E. Sullivan, G.L. Kearns, M.D. Reed, J.D. Marshall, J.N. Van Den Anker, L.P. James, Targeted liquid chromatography-mass spectrometry analysis of serum acylcarnitines in acetaminophen toxicity in children, Biomark. Med. 8 (2014) 147–159.
[2] J.E. Burke, E.A. Dennis, Phospholipase A2 structure/function, mechanism, and signaling, J. Lipid Res. 50 (Suppl) (2009) S237–242.
[3] J. Cheng, X. Ma, K.W. Krausz, J.R. Idle, F.J. Gonzalez, Rifampicin-activated human pregnane X receptor and CYP3A4 induction enhance acetaminophen-induced toxicity, Drug Metab. Dispos. 37 (2009) 1611–1621.
[4] Coen, An integrated metabonomic investigation of acetaminophen toxicity in the mouse using NMR spectroscopy, Chem. Res. Toxicol 16 (2003) 295–303.
[5] Z. Cui, M. Houweling, Phosphatidylcholine and cell death, Biochim. Biophys. Acta 1585 (2002) 87–96.
[6] D.C. Dahlin, G.T. Miwa, A.Y. Lu, S.D. Nelson, N-Acetyl-p-benzoquinone imine: a cytochrome P-450-mediated oxidation product of acetaminophen, Proc. Natl. Acad. Sci. U. S. A. 81 (1984) 1327–1331.
[7] G. Dai, L. He, N. Chou, Y.J. Wan, Acetaminophen metabolism does not contribute to gender difference in its hepatotoxicity in mouse, Toxicol. Sci. 92 (2006) 33–41.
[8] T.J. Davern, L.P. 2nd James, J.A. Hinson, J. Polson, A.M. Larson, R.J. Fontana, E. Lalani, S. Munoz, A.O. Shakil, W.M. Lee, G. Acute Liver Failure Study, Measurement of serum acetaminophen-protein adducts in patients with acute liver failure, Gastroenterology 130 (2006) 687–694.
[9] J.W. Dear, D.J. Antoine, Stratification of paracetamol overdose patients using new toxicity biomarkers: current candidates and future challenges, Expert Rev. Clin. Pharmacol. 7 (2014) 181–189.
[10] K.P. Devi, M. Sreepriya, K. Balakrishna, G. Veluchamy, T. Devaki, Assessment of the protective potential of Premna tomentosa (L. Verbenaceae) extract on lipid profile and lipid-metabolizing enzymes in acetaminophen-intoxicated rats, J. Altern. Complement. Med. (New York, N.Y.) 10 (2004) 540–546.
[11] A. Drzazga, Lysophosphatidylcholine and lysophosphatidylinosiol – novel promissing signaling molecules and their possible therapeutic activity, Acta Pol. Pharm.: Drug Res. 71 (2014) 887–899.

[12] D.L. Eaton, E.P. Gallagher, T.K. Bammler, K.L. Kunze, Role of cytochrome P4501A2 in chemical carcinogenesis: implications for human variability in expression and enzyme activity, Pharmacogenetics 5 (1995) 259–274.
[13] L. Eun-hee, Structure-activity relationship of lysophosphatidylcholines in HL-60 human leukemia cells, Acta Pharmacol. Sin. 25 (2004) 1521–1524.
[14] M. Fukao, Y. Hattori, M. Kanno, I. Sakuma, A. Kitabatake, Structural differences in the ability of lysophospholipids to inhibit endothelium-dependent hyperpolarization by acetylcholine in rat mesenteric arteries, Biochem. Biophys. Res. Commun. 227 (1996) 479–483.
[15] C.R. Gardner, D.E. Heck, C.S. Yang, P.E. Thomas, X.J. Zhang, G.L. DeGeorge, J.D. Laskin, D.L. Laskin, Role of nitric oxide in acetaminophen-induced hepatotoxicity in the rat, Hepatology 27 (1998) 748–754.
[16] F.J. Gonzalez, The 2006 Bernard B. Brodie Award Lecture. Cyp2e1, Drug Metab. Dispos. 35 (2007) 1–8.
[17] N. Hanawa, M. Shinohara, B. Saberi, W.A. Gaarde, D. Han, N. Kaplowitz, Role of JNK translocation to mitochondria leading to inhibition of mitochondria bioenergetics in acetaminophen-induced liver injury, J. Biol. Chem. 283 (2008) 13565–13577.
[18] J.A. Hinson, D.W. Roberts, L.P. James, Mechanisms of acetaminophen-induced liver necrosis, Handb. Exp. Pharmacol. (2010) 369–405.
[19] W.C. Hubbard, A.B. Moser, S. Tortorelli, A. Liu, D. Jones, H. Moser, Combined liquid chromatography-tandem mass spectrometry as an analytical method for high throughput screening for X-linked adrenoleukodystrophy and other peroxisomal disorders: preliminary findings, Mol. Genet. Metab. 89 (2006) 185–187.
[20] T. Illig, C. Gieger, G. Zhai, W. Romisch-Margl, R. Wang-Sattler, C. Prehn, E. Altmaier, G. Kastenmuller, B.S. Kato, H.W. Mewes, T. Meitinger, M.H. de Angelis, F. Kronenberg, N. Soranzo, H.E. Wichmann, T.D. Spector, J. Adamski, K. Suhre, A genome-wide perspective of genetic variation in human metabolism, Nat. Genet. 42 (2010) 137–141.
[21] S. Imhasly, H. Naegeli, S. Baumann, M. von Bergen, A. Luch, H. Jungnickel, S. Potratz, C. Gerspach, Metabolomic biomarkers correlating with hepatic lipidosis in dairy cows, BMC Vet. Res. 10 (2014) 122.
[22] H. Jaeschke, M.R. McGill, A. Ramachandran, Oxidant stress, mitochondria, and cell death mechanisms in drug-induced liver injury: lessons learned from acetaminophen hepatotoxicity, Drug Metab. Rev. 44 (2012) 88–106.
[23] L. James, K. Yan, L. Pence, P. Simpson, S. Bhattacharyya, P. Gill, L. Letzig, G. Kearns, R. Beger, Comparison of bile acids and acetaminophen protein adducts in children and adolescents with acetaminophen toxicity, PLoS One 10 (2015) e0131010.
[24] L.P. James, E.V. Capparelli, P.M. Simpson, L. Letzig, D. Roberts, J.A. Hinson, G.L. Kearns, J.L. Blumer, J.E. Sullivan, Network of Pediatric Pharmacology Research Units, N.I.o.C.H, D. Human, Acetaminophen-associated hepatic injury: evaluation of acetaminophen protein adducts in children and adolescents with acetaminophen overdose, Clin. Pharmacol. Ther. 84 (2008) 684–690.
[25] L.P. James, L. Letzig, P.M. Simpson, E. Capparelli, D.W. Roberts, J.A. Hinson, T.J. Davern, W.M. Lee, Pharmacokinetics of acetaminophen-protein adducts in adults with acetaminophen overdose and acute liver failure, Drug Metab. Dispos. 37 (2009) 1779–1784.
[26] A. Kihara, Very long-chain fatty acids: elongation, physiology and related disorders, J. Biochem. 152 (2012) 387–395.
[27] M. Kim, S. Jung, S.Y. Kim, S.H. Lee, J.H. Lee, Prehypertension-associated elevation in circulating lysophosphatidlycholines, Lp-PLA2 activity, and oxidative stress, PLoS One 9 (2014) e96735.
[28] A. Kleger, S. Liebau, Q. Lin, G. von Wichert, T. Seufferlein, The impact of bioactive lipids on cardiovascular development, Stem Cells Int. 2011 (2011) 916180.
[29] A.M. Larson, J. Polson, R.J. Fontana, T.J. Davern, E. Lalani, L.S. Hynan, J.S. Reisch, F.V. Schiodt, G. Ostapowicz, A.O. Shakil, W.M. Lee, G. Acute Liver Failure Study, Acetaminophen-induced acute liver failure: results of a United States multicenter, prospective study, Hepatology 42 (2005) 1364–1372.
[30] B.H. Lauterburg, Y. Vaishnav, W.G. Stillwell, J.R. Mitchell, The effects of age and glutathione depletion on hepatic glutathione turnover in vivo determined by acetaminophen probe analysis, J. Pharmacol. Exp. Ther. 213 (1980) 54–58.
[31] J. Li, J. Xin, S. Hao, L. Zhang, L. Jiang, D. Chen, Q. Xie, W. Xu, H. Cao, L. Li, Return of the metabolic trajectory to the original area after human bone marrow mesenchymal stem cell transplantation for the treatment of fulminant hepatic failure, J. Proteome Res. 11 (2012) 3414–3422.
[32] J. Ma, J. Yu, X. Su, C. Zhu, X. Yang, H. Sun, D. Chen, Y. Wang, H. Cao, J. Lu, UPLC-MS-based serum metabonomics for identifying acute liver injury biomarkers in Chinese miniature pigs, Toxicol. Lett. 225 (2014) 358–366.
[33] A. Michaut, C. Moreau, M.A. Robin, B. Fromenty, Acetaminophen-induced liver injury in obesity and nonalcoholic fatty liver disease, Liver Int. 34 (2014) e171–179.
[34] K.L. Muldrew, L.P. James, L. Coop, S.S. McCullough, H.P. Hendrickson, J.A. Hinson, P.R. Mayeux, Determination of acetaminophen-protein adducts in mouse liver and serum and human serum after hepatotoxic doses of acetaminophen using high-performance liquid chromatography with electrochemical detection, Drug Metab. Dispos. 30 (2002) 446–451.
[35] A.D. Patterson, Y.M. Shah, T. Matsubara, K.W. Krausz, F.J. Gonzalez, Peroxisome proliferator-activated receptor alpha induction of uncoupling protein 2 protects against acetaminophen-induced liver toxicity, Hepatology 56 (2012) 281–290.
[36] Y. Qiu, L.Z. Benet, A.L. Burlingame, Identification of the hepatic protein targets of reactive metabolites of acetaminophen in vivo in mice using two-dimensional gel electrophoresis and mass spectrometry, J. Biol. Chem. 273 (1998) 17940–17953.
[37] B.H. Rumack, Acetaminophen overdose in young children: treatment and effects of alcohol and other additional ingestants in 417 cases, Am. J. Dis. Child. 138 (1984) 428–433.
[38] M.M. Rumore, R.G. Blaiklock, Influence of age-dependent pharmacokinetics and metabolism on acetaminophen hepatotoxicity, J. Pharm. Sci. 81 (1992) 203–207.
[39] T. Sassa, A. Kihara, Metabolism of very long-chain Fatty acids: genes and pathophysiology, Biomol. Ther. 22 (2014) 83–92.
[40] L.E. Schmidt, Age and paracetamol self-poisoning, Gut 54 (2005) 686–690.
[41] R.B. Schutgens, I.W. Bouman, A.A. Nijenhuis, R.J. Wanders, M.E. Frumau, Profiles of very-long-chain fatty acids in plasma, fibroblasts, and blood cells in Zellweger syndrome, X-linked adrenoleukodystrophy, and rhizomelic chondrodysplasia punctata, Clin. Chem. 39 (1993) 1632–1637.
[42] A.M. Sheikh, M. Michikawa, S.U. Kim, A. Nagai, Lysophosphatidylcholine increases the neurotoxicity of Alzheimer's amyloid beta1-42 peptide: role of oligomer formation, Neuroscience 292 (2015) 159–169.
[43] K.S. Shivashangari, V. Ravikumar, T. Devaki, Evaluation of the protective efficacy of Asteracantha longifolia on acetaminophen-induced liver damage in rats, J. Med. Food 7 (2004) 245–251.
[44] J.E. Vance, D.E. Vance, Metabolic insights into phospholipid function using gene-targeted mice, J. Biol. Chem. 280 (2005) 10877–10880.
[45] K. Varmuza, P. Filzmoser, Introduction to Multivariate Statistical Analysis in Chemometrics, Taylor & Francis-CRC Press, FL, USA, 2009.
[46] B.H. Walsh, D.I. Broadhurst, R. Mandal, D.S. Wishart, G.B. Boylan, L.C. Kenny, D.M. Murray, The metabolomic profile of umbilical cord blood in neonatal hypoxic ischaemic encephalopathy, PLoS One 7 (2012) e50520.
[47] L. Whiley, A. Sen, J. Heaton, P. Proitsi, D. Garcia-Gomez, R. Leung, N. Smith, M. Thambisetty, I. Kloszewska, P. Mecocci, H. Soininen, M. Tsolaki, B. Vellas, S. Lovestone, C. Legido-Quigley, Evidence of altered phosphatidylcholine metabolism in Alzheimer's disease, Neurobiol. Aging 35 (2014) 271–278.
[48] L. Zhao, G. Pickering, Paracetamol metabolism and related genetic differences, Drug Metab. Rev. 43 (2011) 41–52.